*Human Molecular Genetics, 2014, Vol. 23, No. 23* **6177–6190**
*doi:10.1093/hmg/ddu338*
*Advance Access published on July 2, 2014*

# Neural deletion of Tgfbr2 impairs angiogenesis through an altered secretome

**Nicole Hellbach[1,2], Stefan C. Weise[1,2], Riccardo Vezzali[1,2], Shalaka D. Wahane[1,2], Stefanie Heidrich[1], Deborah Roidl[1], Jan Pruszak[3,4], Jennifer S. Esser[5] and Tanja Vogel[1,*]**

[1]Department of Molecular Embryology, Institute of Anatomy and Cell Biology, University of Freiburg, 79104 Freiburg, Germany, [2]Faculty of Biology, University of Freiburg, 79104 Freiburg, Germany, [3]Emmy Noether-Group for Stem Cell Biology, Department of Molecular Embryology, Institute of Anatomy and Cell Biology, University of Freiburg, 79104 Freiburg, Germany, [4]Center for Biological Signaling Studies (BIOSS), University of Freiburg, 79104 Freiburg, Germany and [5]Department of Cardiology and Angiology I, University Heart Center Freiburg, 79106 Freiburg, Germany

Received May 26, 2014; Revised May 26, 2014; Accepted June 26, 2014

**Simultaneous generation of neural cells and that of the nutrient-supplying vasculature during brain development is called neurovascular coupling. We report on a transgenic mouse with impaired transforming growth factor β (TGFβ)-signalling in forebrain-derived neural cells using a *Foxg1-cre* knock-in to drive the conditional knock-out of the *Tgfbr2*. Although the expression of FOXG1 is assigned to neural progenitors and neurons of the telencephalon, *Foxg1*$^{cre/+}$;*Tgfbr2*$^{flox/flox}$ (Tgfbr2-cKO) mutants displayed intracerebral haemorrhage. Blood vessels exhibited an atypical, clustered appearance were less in number and displayed reduced branching. Vascular endothelial growth factor (VEGF) A, insulin-like growth factor (IGF) 1, IGF2, TGFβ, inhibitor of DNA binding (ID) 1, thrombospondin (THBS) 2, and a disintegrin and metalloproteinase with thrombospondin motifs (ADAMTS) 1 were altered in either expression levels or tissue distribution. Accordingly, human umbilical vein endothelial cells (HUVEC) displayed branching defects after stimulation with conditioned medium (CM) that was derived from primary neural cultures of the ventral and dorsal telencephalon of Tgfbr2-cKO. Supplementing CM of Tgfbr2-cKO with VEGFA rescued these defects, but application of TGFβ aggravated them. HUVEC showed reduced migration towards CM of mutants compared with controls. Supplementing the CM with growth factors VEGFA, fibroblast growth factor (FGF) 2 and IGF1 partially restored HUVEC migration. In contrast, TGFβ supplementation further impaired migration of HUVEC. We observed differences along the dorso-ventral axis of the telencephalon with regard to the impact of these factors on the phenotype. Together these data establish a TGFBR2-dependent molecular crosstalk between neural and endothelial cells during brain vessel development. These findings will be useful to further elucidate neurovascular interaction in general and to understand pathologies of the blood vessel system such as intracerebral haemorrhages, hereditary haemorrhagic telangiectasia, Alzheimer's disease, cerebral amyloid angiopathy or tumour biology.**

## INTRODUCTION

Transforming growth factor β (TGFβ)-signalling is important for development in mice as various null deletions of TGFβ-ligands and -receptors lead to embryonic and postnatal death (1,2). TGFβ ligands 1–3 initiate a canonical downstream signalling through high-affinity binding to TGFβ receptor 2 (TGFBR2). This results in the recruitment and subsequent transphosphorylation of TGFBR1, which in turn activates associated SMAD proteins (3,4). In addition, TGFβ is capable to activate other, non-Smad intracellular pathways. Owing to its pleiotropic effects and importance for general development, disturbed TGFβ-signalling has various phenotypic consequences like

*To whom correspondence should be addressed. Tel: +49 7612035086, Fax: +49 7612035091; E-mail: tanja.vogel@anat.uni-freiburg.de.

neoplastic transformations, deregulation of immune cells as well as defects in distinct organs (2,5–7). The cardiovascular system is very sensitive to the loss of TGFβ-signalling as knock-outs in mouse models for *Tgfβ1-3*, *Activin A receptor type II-like 1* (*Acvrl1/Alk1*), *TGFβ-receptor I* (*Tgfbr1/Alk5*), *Tgfbr2* and *Endoglin* (*Eng*) all display an abnormal vasculature (8,9). In addition, patients presenting vascular malformations in Marfan's or Loeys–Dietz syndrome, with intracerebral haemorrhages (ICHs) or haemorrhagic hereditary telangiectasia (HHT), have mutations in *ALK1*, *ALK5*, *ENG*, *SMAD4*, *TGFBR1* or *-2* (9–12). It is currently under investigation whether TGFβ can serve as a biomarker for ICH that is observed in preterm infants (13,14). ICH in patients presenting also with arteriovenous malformations is frequently associated with single nucleotide polymorphism in *TGFBR2* (15). Overproduction of TGFβ seems to be a predisposing factor for amyloid deposition that is observed in patients with Alzheimer's disease or cerebral amyloid angiopathy (CAA). This finding is corroborated in mice in which overexpression of TGFβ1 in astrocytes led to a thickening of the basal membrane through overproduction of extracellular matrix (ECM) specifically around vessels of the cerebral cortex (16). However, the molecular mechanisms that lead to the various phenotypes are not fully understood yet. This is partly because TGFβ-signalling in endothelial cells (EC) is diverse and context-dependent. One example is that TGFβ is able to activate two distinct type I receptors in EC, i.e. ALK1 and ALK5. Via ALK1, TGFβ induces phosphorylation of SMAD1/5 and via ALK5 SMAD2/3 phosphorylation (17). The cellular read-out of these activations is context-dependent. In mouse embryonic endothelial cells (MEEC) activation of ALK5-dependent signalling results in impaired migration and proliferation. In contrast, ALK1 activity leads to increased cell migration and proliferation (18). Another study investigated constitutive ALK1 activity in human microvascular endothelial cells from the dermis and observed increased cell proliferation and decreased migration (19). Furthermore, TGFβ-signalling in EC is modulated through the expression of ENG. ENG binds to the ligands TGFβ1 and 3 in the presence of TGFBR2. In MEEC, ENG promotes proliferation and migration via TGFβ–ALK1 signalling (20). However, ENG-deficient MEEC show increased proliferation rates and ALK1 activation (21). Another layer of complexity of TGFβ-signalling is that TGFβ affects EC in a concentration-dependent manner, whereby low concentrations promote whereas higher inhibit angiogenesis (22,23). The TGFβ-signalling read-out is also modulated by other molecules such as Cadherin-5 (CDH5) (22). In addition, TGFβ crosstalks to a variety of different other signalling pathways, e.g. inhibition of TGFβ-signalling alongside with activation of vascular endothelial growth factor (VEGF), efficiently promotes EC-sprouting and -migration (24).

In further attempts aiming to unravel TGFβ-function in the vasculature, several mouse models were studied in which the TGFβ pathway was disrupted specifically in EC (8). Ablation of SMAD4 in EC impairs TGFβ-Notch crosstalk. This leads to loss of Cadherin-2 (CDH2) expression, which is a neural adhesion protein necessary for recruitment of pericytes and subsequent vessel stabilization (25). In the eye and cerebral cortex, EC-specific inactivation of *Tgfbr2* leads to the formation of EC clusters, with impaired migration into the neural parenchyma. However, EC still recruit pericytes and form proper cell–cell contacts (26). Orphan G protein-coupled receptor *Gpr124* is expressed in cerebral EC and pericytes. GPR124-deficient vasculature also forms EC clusters, resembling those reported after EC-specific *Tgfbr2* inactivation (27,28). *Gpr124* expression is increased after TGFβ1 stimulation, and deletion of *Gpr124* increases the expression of TGFβ itself as well as of several TGFβ target genes (27,29).

Our aim is to understand the partially known role of TGFβ in the development of the central nervous system (CNS). Different attempts show so far that TGFβ is anti-mitotic and mediates neural differentiation in the cerebral cortex and hippocampus (30–33). In the midbrain, TGFβ is implicated in the generation and survival of dopaminergic neurons (34). In this study, we used a *Foxg1-cre* knock-in to inactivate *Tgfbr2* in the developing forebrain to further reveal the influence of TGFβ-signalling on cortical development (35). The transcription factor FOXG1 is required for the development of the dorsal (DT) as well as ventral telencephalon (VT). *Foxg1*-deficient mice display a dramatically reduced forebrain, and the animals die prenatally. *Foxg1* is transcribed in the neural tube from E8.5 onwards (36). In the DT, it has important functions in neural progenitors and neurons of the cortical plate (37). Here, it influences progenitor proliferation, neuronal specification by suppression of cortical hem, Cajal–Retzius cell fates and migration of pyramidal neurons in the cortical plate (38). FOXG1 is also necessary for the expression of ventral marker genes and therefore contributes to the specification of the VT as well (39). In the VT however, loss of FOXG1 does not influence cell proliferation, indicating that FOXG1 exerts different functions along the dorso-ventral axis. Surprisingly, in the mouse model described here, the simultaneous partial reduction of FOXG1 and deletion of *Tgfbr2* resulted in severe ICH. This has not been observed in any other neuroepithelial-specific *Tgfbr2* deletion (this study, 40,41). We identified that the ICH developed through disturbed neural secretion, expression and reduced bioavailability of the signalling molecules VEGFA, fibroblast growth factor (FGF) 2, insulin-like growth factor (IGF) 1, -2 and TGFβ and are associated with altered expression of the inhibitor of DNA binding (ID) 1, as well as the proteins involved in cell–cell and cell–matrix interaction, namely thrombospondin (THBS) 2 and a disintegrin and metalloproteinase with thrombospondin motifs (ADAMTS) 1.

## RESULTS

### Deletion of *Tgfbr2* in neural cells results in intracerebral haemorrhages in the telencephalon

To study the influence of TGFβ-signalling on cortical development, we generated $Foxg1^{cre/+};Tgfbr2^{flox/flox}$ (Tgfbr2-cKO) embryos that showed massive ICH from E12.5 onwards (Supplementary Material, Fig. S1A), mostly affecting the VT (Fig. 1Ad–f, yellow arrow). Haemorrhages became more pronounced with development (Supplementary Material, Fig. S1A), and erythrocytes infiltrated also the DT. At later stages, we observed intraventricular blood leakage (Supplementary Material, Fig. S1Af, h, yellow arrowheads). In several cases, haemorrhages extended into the di- and mesencephalon (Fig. 1Ae). In contrast, other *Tgfbr2* conditional deletions targeting cells of neural lineages using *Gfap-cre* and *Nestin-cre*

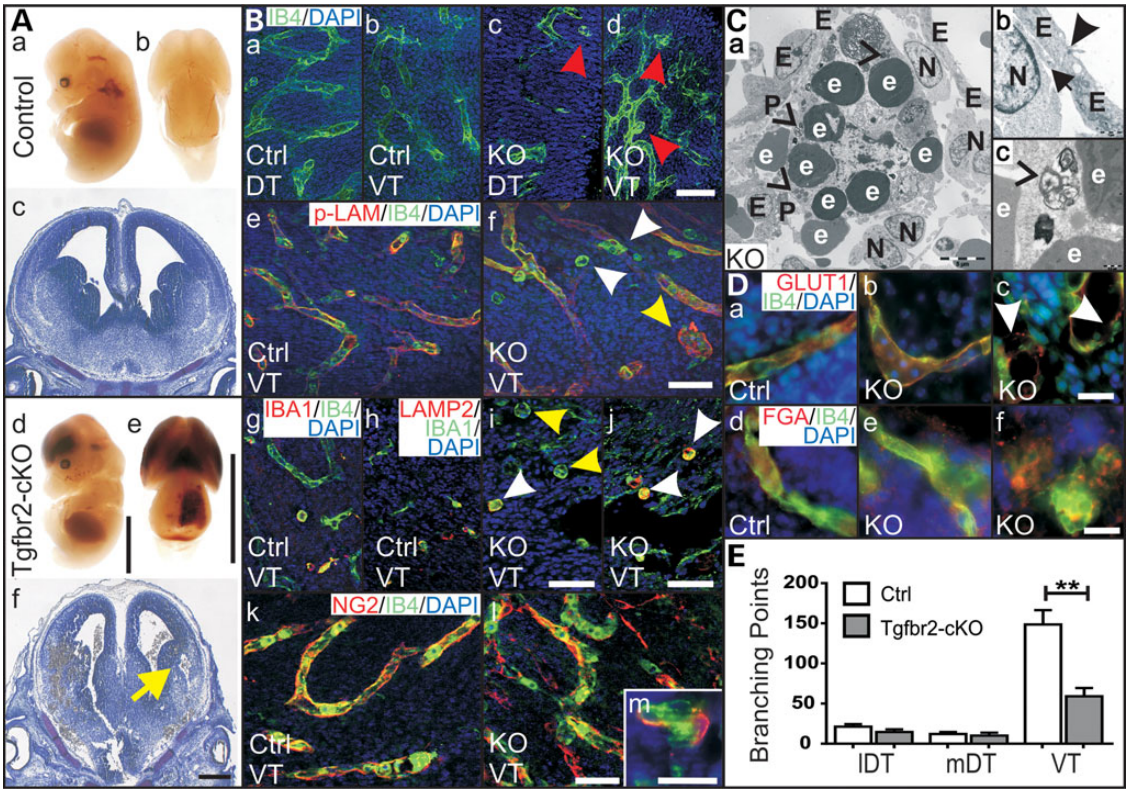


**Figure 1.** Conditional deletion of *Tgfbr2* impaired angiogenesis and showed prominent ICH. (**A**) (a–f) Tgfbr2-cKO displayed haemorrhages in the CNS at E14.5 compared with controls, mostly in VT (yellow arrows). (**B**) (a–d) IB4-positive cells appeared in clusters at E13.5 in VT of Tgfbr2-cKO (red arrow heads), but not of controls. (e–j) Some clusters contained a basal lamina (p-LAM-/IB4-positive, yellow arrow heads); some were activated microglia cells (IBA1/LAMP2-positive, white arrow heads). (k–m) NG2-positive pericytes covered vessels and EC clusters. (**C**) (a–c) EM of Tgfbr2-cKO (E12.5) showed phagocytic cells in VT. Phagocytosis of extravascular erythrocytes (e) was displayed by different digestion stages and vesicular structures (black hollow arrowheads, a, c). EC (E) were covered by pericytes (P) and basal lamina (black arrow). They were connected by cell junctions (black arrowheads). ECM and neural cells (N) were less dense around vessels. (**D**) (a–f) Discontinued GLUT1 expression (white arrow heads) and extravascular fibrinogen (FGA) in EC clusters of Tgfbr2-cKO in VT showed permeability of vessels. FGA was localized intravascular in normal vessels of Tgfbr2-cKO and control. (**E**) Less branching points were detected in VT of Tgfbr2-cKO compared with controls at E13.5 ($n = 3$). lDT: lateral dorsal telencephalon; mDT: medial DT; VT, ventral telencephalon; scale bars: 500 μm (Aa, b, d, e), 200 μm (Ac, f), 50 μm (B), 5 μm (Ca), 1 μm (Cb), 0.5 μm (Cc) and 20 μm (Bm, D).

displayed a normal brain vasculature (Supplementary Material, Fig. S1B and C).

We hypothesized that *Tgfbr2* deletion could occur in EC although FOXG1 expression has so far mainly been assigned to neural cells. We did not observe expression of CRE recombinase in EC and pericytes of Tgfbr2-cKO (Supplementary Material, Fig. S2A), and immunostaining for CRE was only positive in neural cells (Supplementary Material, Fig. S2Ad). This finding was confirmed through analysis of a GFP-reporter mouse line in which we did not observe co-localization of GFP and vessel markers CD31 and SMA (Supplementary Material, Fig. S2Ba, b). Further, *Foxg1* expression was nearly undetectable in RNA isolated from primary mouse embryonic brain EC (Supplementary Material, Fig. S2Bc). Accordingly, we confirmed reduction of TGFBR2 in the neural tissue of Tgfbr2-cKO by qRTPCR, immunoblotting and immunostaining of tissue sections as well as of cultured neural cells (Supplementary Material, Fig. S2Ca–i). The latter revealed that these primary cell cultures contained TGFBR2-deficient as well as normal TGFBR2-expressing cells (Supplementary Material, Fig. S2Cc–f). In addition, *Foxg1* mRNA was also reduced in these mutants as expected for heterozygote *Foxg1-cre* mice (42) (Supplementary Material, Fig. S2Cg). These data suggested that either the simultaneous reduction of TGFBR2 and FOXG1 is responsible for the observed phenotype or the spatio-temporal specificities of FOXG1 that drives CRE expression. We analysed the vessel morphology of homozygote *Foxg1-cre* mice, i.e. in a *Foxg1*-null mouse line at E13.5. Single *Foxg1*-deficient forebrains were reduced in size. However, they did not display any angiogenic defect (Supplementary Material, Fig. S1Dc, g). To analyse whether complete loss of TGFBR2 and FOXG1 would produce a more severe phenotype, we extended our analysis to double mutant (dKO) mice. dKO forebrains displayed vascular defects alongside with a reduction in brain size (Supplementary Material, Fig. S1Dd, h), which indicates an additive phenotype compared with the single mutants. The vascular phenotype did not appear to be more severe in dKO compared with Tgfbr2-cKO. We hypothesized that a more severe phenotype might be observable at earlier developmental time points. To test this, we analysed the different mutant strains at E11.5 (Supplementary Material, Fig. S1Ea–h). All mutant animals had sporadic, mild alterations in the vascular structures compared with control animals (Supplementary Material, Fig. S1Ef–h, red arrowheads), but we could not detect an earlier onset of vascular malformation in dKO that would be comparable to Tgfbr2-cKO mice. Together these data indicated that reduction

of FOXG1 alone does not result in a vascular phenotype, which is therefore more likely produced by simultaneous reduction of TGFBR2 and FOXG1. To further extend these analyses, we refer to an *Emx1-cre*-driven *Tgfbr2* deletion that did not result in abnormal brain vessels ((40) and our own observations). Watanabe *et al*. reported that EMX1 and FOXG1 are co-expressed in cortical cells (43) and we confirmed these results by showing that in cultured neural cells from Tgfbr2-cKO animals, >95% of cells were positive for both EMX1 and CRE (Supplementary Material, Fig. S2Da–d). The overlap between NESTIN- and CRE-positive cells was less, i.e. 36% in VT- and 53% in DT-derived cells (Supplementary Material, Fig. S2De–h). From these data, we conclude that the phenotype observed in *Foxg1-cre*-driven *Tgfbr2* deletion results from simultaneous reduction in FOXG1 and TGFBR2 rather than exclusively from a reduction of TGFBR2 in a specific FOXG1- and EMX1-positive cell type.

### Vessel morphology and blood–brain barrier integrity is disturbed in Tgfbr2-cKO

To investigate the origin of haemorrhages, we characterized the vasculature of Tgfbr2-cKO. Flow cytometry revealed unchanged EC numbers in the entire mutant forebrain (Supplementary Material, Fig. S3A), and investigation of active CASP3 did not indicate increased apoptosis (Supplementary Material, Fig. S3C). Apart from normal vessels with a tubular structure, mutant brains displayed impaired vascular structures that appeared in EC clusters. These clusters were localized predominantly in the VT but appeared in later developmental stages in the DT as well (Fig 1Bc, d, red arrowheads), and their localization within the brain parenchyma correlated with the CRE-expression domain (Supplementary Material, Fig. S3B). Clustered malformations affected veins and arteries without preference (Supplementary Material, Fig. S3Ec, e, f). Some clusters contained a basal lamina, but others were negative for pan-Laminin (Fig. 1Bf, yellow and white arrowheads). Several clusters stained positive for the microglial marker IBA1 and showed signs of active phagocytosis (Fig. 1Bi, j, white arrowheads), which was also corroborated by flow cytometry (Supplementary Material, Fig. S3A). Electron microscopy (EM) confirmed phagocytic cells close to vessels that mainly contained erythrocytes (Fig. 1C and Supplementary Material, Fig. S4). In summary, these data identified an angiogenesis defect with clustered IB4-positive EC as well as activated, clustered microglia in Tgfbr2-cKO.

ECM that surrounded leaky vessels appeared less dense in Tgfbr2-cKO than that in control brains (Fig. 1C and Supplementary Material, Fig. S4Bb, e), but changes in collagen and proteoglycan content or in fibronectin expression could not be detected (Supplementary Material, Fig. S5A). We assumed that a less dense ECM might be indicated by a reduced number of cells that are localized within the vascular niche. Recently published data indicate a close association between the vasculature and cortical progenitors that express *Eomes*, a T-box transcription factor (44). Accordingly, we quantified the EOMES-expressing progenitors in a distance of 20 μm around the vessel. Tgfbr2-cKO contained less EOMES-positive cells in this vascular niche, albeit overall numbers of EOMES cells remained unchanged compared with controls (Supplementary Material, Fig. S3F). Blood–brain barrier (BBB)-specific structures such as tight junctions (CLDN5, CLDN12 and ZO1) and adherens junctions (CDH5 and CDH2) were unaltered in Tgfbr2-cKO vessels compared with controls (Supplementary Material, Fig. S3D). GLUT1 expression appeared discontinued in EC clusters (Fig. 1Dc), and extravascular Fibrinogen (Fig. 1Df) confirmed permeability and/or improper BBB development. Together, these data showed in addition to clustered EC, less dense ECM, a disturbed vascular niche and BBB permeability in Tgfbr2-cKO.

### Pericyte recruitment is normal but vascular branching is reduced in Tgfbr2-cKO

Impaired TGFβ-signalling in EC can have influence on EC-associated mural cells, e.g. smooth muscle cells and pericytes. TGFβ can be implicated in recruitment, association or proliferation of these mural cells (8). In the brain, an EC-specific *Smad4*-knock-out resulted in vessel malformations through a defect in pericyte recruitment that caused haemorrhages (25). Immunostainings, flow cytometry and EM revealed that in Tgfbr2-cKO pericytes were present on tube-forming vessels and appeared normal in shape and coverage (Fig. 1Bk, l, Supplementary Material, Fig. S3A, S4). EC clusters also contained pericytes (Fig. 1Bm). We concluded that a disturbed EC–pericyte interaction might not be the cause for the observed phenotype. In contrast, quantitative analyses of vessel branching points revealed a defect from E13.5 onwards that aggravated over time, such that at E14.5, the VT of Tgfbr2-cKO contained significantly fewer vessels (Fig. 1E, Supplementary Material, Fig. S5Cc, d, S5Dc, d). Together these data indicated that initial specification and development of vessels was not disturbed in Tgfbr2-cKO and that pericytes were recruited normally. However, the vascular defect in Tgfbr2-cKO developed through signals from neural cells that appeared from around E12.5 onwards.

### Expression of pro- and anti-angiogenic factors is altered in Tgfbr2-cKO

To gain further insight into molecular mechanisms implicated in abnormal angiogenesis in Tgfbr2-cKO, we specifically analysed expression of (1) soluble factors produced by neural cells, which influence angiogenesis (VEGFA, FGF2, IGF1 and -2, IGFBPs, TGFβ); (2) a TGFβ target gene, which influences angiogenesis (ID1) and (3) proteins present on an angiogenesis protein array (AP-array) (e.g. THSB2 and ADAMTS1). Total expression of VEGFA isoforms did not change either on protein or mRNA levels in whole forebrain tissue samples and in neural cells that we cultured until DIV4 and 12, respectively (Fig. 2B, Supplementary Material, Fig. S6Aa–f). However, VEGFA appeared in protein aggregates in stained sections of Tgfbr2-cKO (Fig. 2Aa, b). These aggregates were enriched in all forebrain regions and mainly localized outside of vessels within the brain parenchyma (Fig. 2C, Supplementary Material, Fig. S6Ai). We detected aggregates already at E11.5 and E12.5 in Tgfbr2-cKO forebrains (Supplementary Material, Fig. S6Ag, h). We hypothesized that although expression levels of VEGFA did not change, altered VEGFA protein localization could be implicated in the observed phenotype of Tgfbr2-cKO. IGF1 and -2 protein levels were significantly increased in whole brain extracts (Fig. 2Ac–f, and B). On the

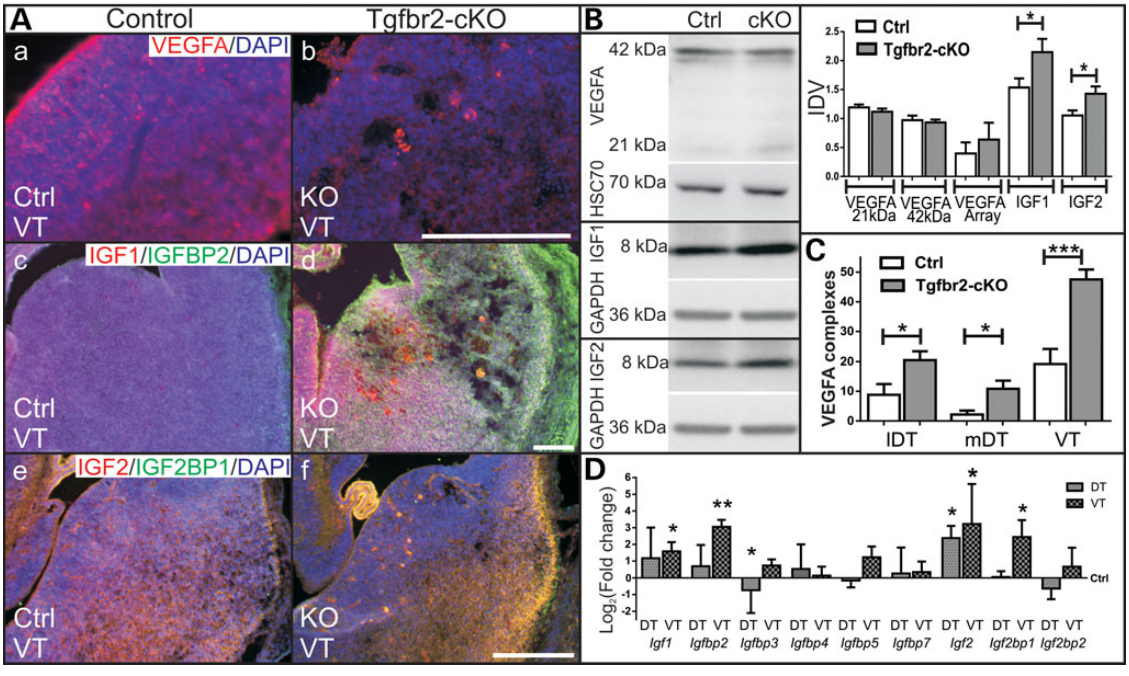


**Figure 2.** Altered expression of VEGFA, IGF1, -2 and IGF-binding proteins. (**A**) (a–b) VEGFA accumulated in E13.5 Tgfbr2-cKO compared with controls. (c–f) IGF1, -2, IGFBP2 and IGF2BP1 expression increased in Tgfbr2-cKO. (**B**) Immunoblot and densitometric analyses revealed unchanged VEGFA isoform (21 and 42 kDa) expression in protein extracts from forebrains of Tgfbr2-cKO compared with controls at E13.5 ($n = 7$). AP-array confirmed unchanged VEGFA protein levels in lysed hemispheres of E13.5 control and mutant embryos ($n = 2$). Immunoblots and densitometric analyses revealed increased IGF1 ($n = 7$) and IGF2 ($n = 4$) expression in Tgfbr2-cKO forebrains at E13.5 compared with control forebrain lysates. (**C**) Quantification revealed an increased amount of VEGFA complexes in Tgfbr2-cKO compared with controls in lDT, mDT and VT at E13.5. (**D**) qRTPCR of cultivated cells from E13.5 DT and VT showed increased *Igf1*, *-bp2* and *Igf2bp1* in VT and reduced *Igfbp3* expression in DT ($n = 3$). $Log_2$ of the fold change is given compared with control. IDV, integrated density value; scale bar: 200 μm.

mRNA level, we corroborated significantly higher IGF1 expression in neurons cultured from the VT until DIV12 and higher IGF2 expression from the VT and DT of Tgfbr2-cKO (Fig. 2D). qRTPCR further revealed higher expression of *Igfbp2* and *Igf2bp1* in VT-derived cultured cells of Tgfbr2-cKO compared with controls (Fig. 2D). *Igfbp3*-mRNA expression was reduced in cultured cells from the DT of Tgfbr2-cKO, although its expression level was unchanged on protein level (Fig. 2D, Supplementary Material, Fig. S6Bg, h). Immunostainings for IGF1 and -BP2 revealed that both proteins only partially co-localized in the VT of control and Tgfbr2-cKO hemispheres, albeit IGF2 overlapped substantially with IGF2BP1 in the VT (Fig. 2Ac–f). These data suggested that although amounts of IGF1 and -2 were increased in VT of Tgfbr2-cKO, their bioavailability might be limited owing to increased IGFBP2 and IGF2BP1 production.

Protein levels of FGF2 were unchanged, but we observed focal accumulation predominantly in microglia (Supplementary Material, Fig. S6Ba–f, white arrowheads). Stalk cells are the trailing proliferating EC that follow the guiding tip cell during migration (45). ID-proteins influence neuro- and angio genesis (46) and are expressed in EC especially by stalk cells. They can be repressed through TGFβ (47,48). ID1 is also a downstream target of bone morphogenic protein (BMP)-signalling, which is implicated in EC migration and tube formation (49). ID1 protein levels were increased in Tgfbr2-cKO (Fig. 3D–F). Moreover, immunostainings indicated ID1-positive EC in controls and mutants as well as in EC clusters showing presence of stalk cells within these structures (Fig. 3E and F). JAG1, another stalk cell marker, as well as the tip cell marker DLL4, were normally expressed in Tgfbr2-cKO (Supplementary Material, Fig. S7a, b), although DLL4 was slightly decreased in the AP-array (Supplementary Material, Fig. S6Ca, S7c–f). We concluded that tip and stalk cells are correctly specified in Tgfbr2-cKO. THBS2 and ADAMTS1 are also known to influence angiogenesis and ECM remodelling (50–52). Expression levels of both proteins were lower in Tgfbr2-cKO compared with controls (Fig. 4). These data further corroborated a molecular basis of our EM-based findings regarding an altered ECM in Tgfbr2-cKO.

## Cultured Tgfbr2-cKO primary neural cells secrete less VEGFA but more TGFβ

*In vivo* analyses had suggested that sprouting and migration defects could be caused by altered localization and/or bioavailability of soluble and ECM-organizing factors in Tgfbr2-cKO. To confirm that neural cells produced these factors, which in turn acted on EC during brain development, we analysed conditioned medium (CM) that we harvested from primary neural cells. We isolated cells from the DT or VT of Tgfbr2-cKO as well as controls and confirmed separation of the two regions by PAX6 staining (Supplementary Material, Fig. S8A). ELISA of CM from both sources revealed significantly less VEGFA in medium derived from Tgfbr2-cKO (Fig. 5A). We detected similar levels of IGF1, -2 as well as FGF2 secretion in mutant and control CM (Supplementary Material, Fig. S8Ba–f). However, we did not observe alterations in VEGFA, IGF1 or

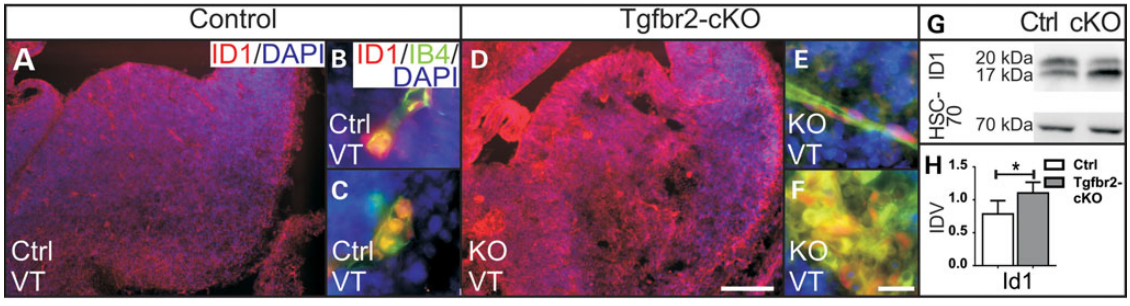


**Figure 3.** Increased ID1 expression in Tgfbr2-cKO. (A–H) Staining, immunoblot and densitometric analyses at E13.5 in Tgfbr2-cKO ($n = 5$). Normal vessels and EC cluster of Tgfbr2-cKO contained ID1-positive cells. Scale bars: 200 μm (A, D) and 20 μm (B–F).

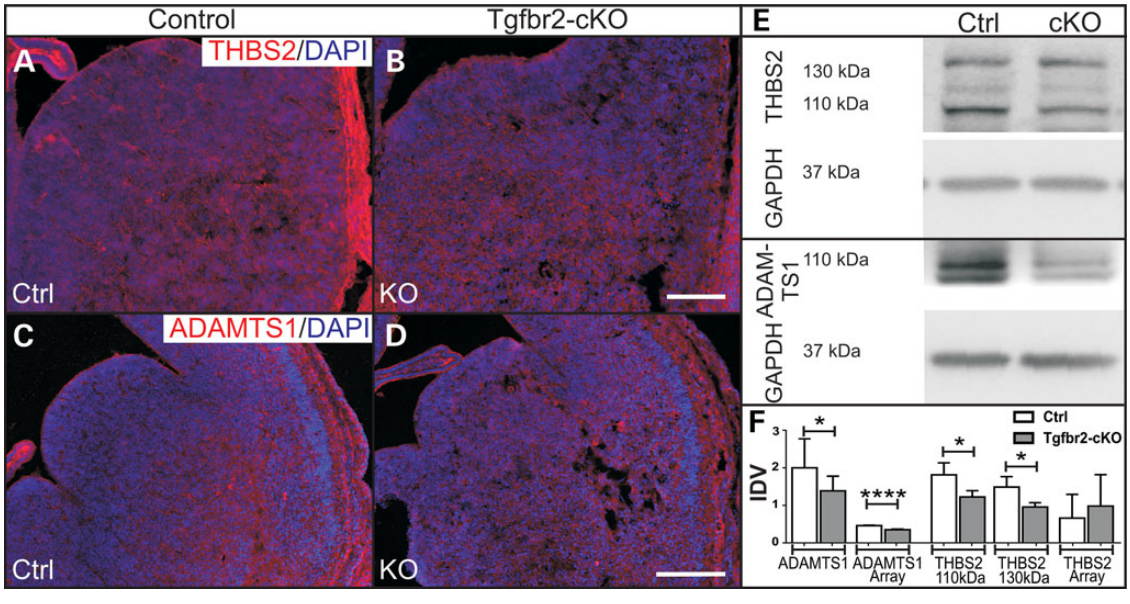


**Figure 4.** Decreased expression of THBS2 and ADAMTS1 in Tgfbr2-cKO. (A–D) Staining for THBS2 and ADAMTS1 showed reduced expression in forebrains of Tgfbr2-cKO at E13.5. (E and F) Immunoblots and densitometric analyses of THBS2 ($n = 3$) and ADAMTS1 ($n = 9$) confirmed reduced THBS2 and ADAMTS1 expression in Tgfbr2-cKO at E13.5. AP-array ($n = 2$) revealed reduced ADAMTS1. Scale bar: 200 μm.

FGF2 levels when we analysed proteins from total forebrain extracts (Supplementary Material, Fig. S8C). TGFβ secretion was significantly increased in DT-derived CM of Tgfbr2-cKO cells (Fig. 5B), but we did not observe significant differences of TGFβ in VT-derived CM. VEGFA aggregates also formed in cultured neural cells similar to our observation in forebrain tissue sections, which suggested that *in vitro* studies are eligible to characterize the molecular origin of the phenotype in further detail. Therefore, we used *in vitro* cultivated neural cells from the DT and VT to analyse the reason for diminished VEGFA secretion. Co-staining of VEGFA and the Golgi marker GM130 revealed that most VEGFA in Tgfbr2-cKO-derived cells localized in the Golgi (Fig. 5D and F). In control cells, however, VEGFA also localized outside of the Golgi (Fig. 5C and E, white arrowheads). We conclude that VEGFA is trapped in the Golgi and is therefore secreted less in Tgfbr2-cKO. To support the finding that impaired VEGFA secretion is dependent on the simultaneous decrease in FOXG1 and TGFBR2 expression, we applied an shRNA-mediated knock-down of FOXG1 and TGFBR2 in WT cortical cells. Lentiviral delivery of shRNA against *Foxg1*, *Tgbr2* or the combination of both reduced expression of either *Foxg1* or *Tgfbr2* with the specific shRNAs and of both genes when the combination was used (Fig. 5H and I). Using this approach, we analysed VEGFA secretion at DIV16 in the different shRNA interference conditions (Fig. 5G). These experiments showed that only the simultaneous knock-down of both factors resulted in a significant reduction of VEGFA secretion, whereas single knock-downs did not change the levels significantly (Fig. 5G). These observations therefore corroborated the hypothesis that simultaneous reduction of FOXG1 and TGFBR2, at least in part, led to the observed phenotype.

## Vascular branching defects result from impaired VEGFA and TGFβ secretion

To further extend our analysis of the molecular origin of the Tgfbr2-cKO phenotype, we used human umbilical vein endothelial cells (HUVEC) to investigate the influence of CM on endothelial cell branching and migration. HUVEC have been used in different studies to unravel general effects of brain vessel

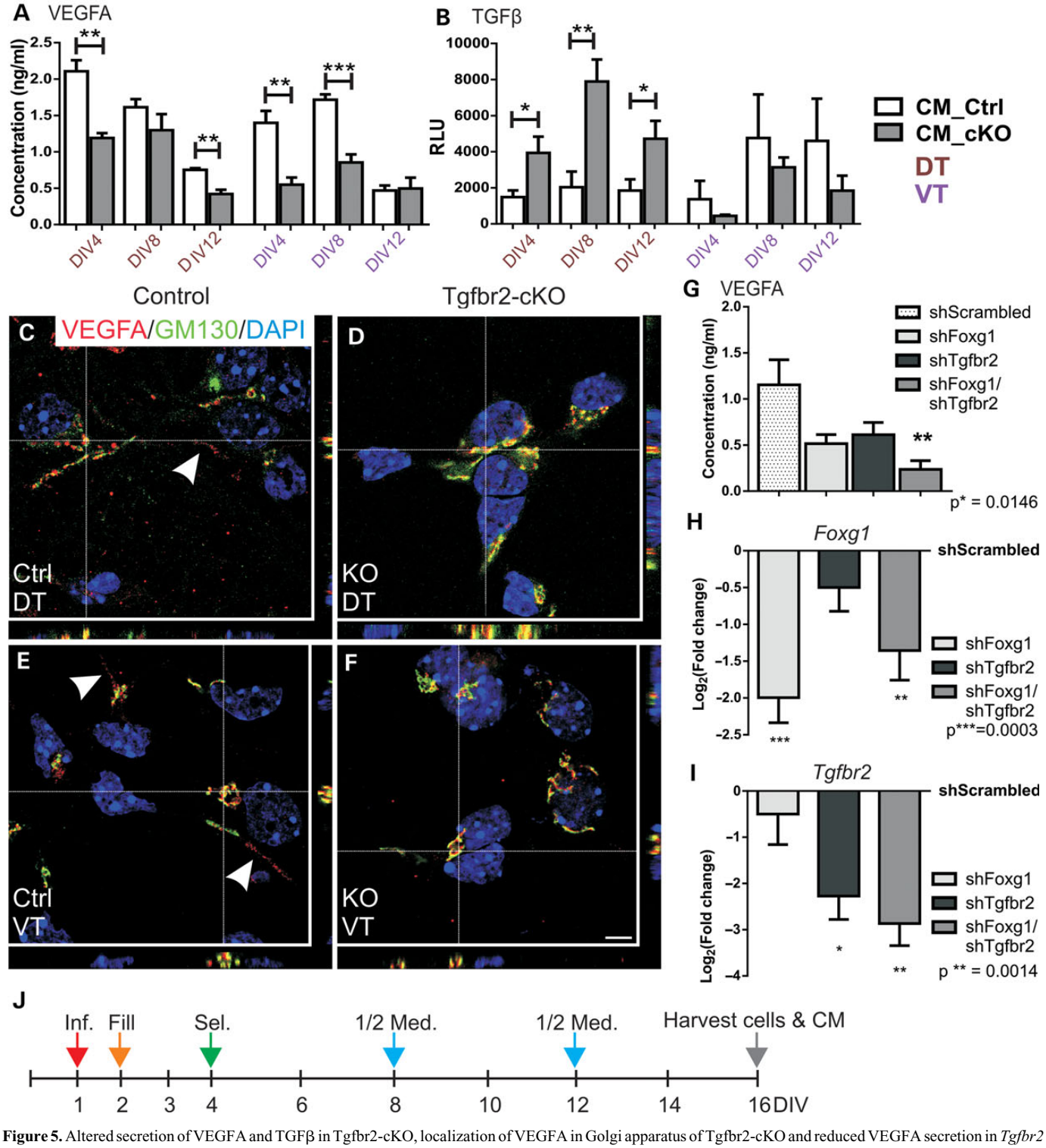


**Figure 5.** Altered secretion of VEGFA and TGFβ in Tgfbr2-cKO, localization of VEGFA in Golgi apparatus of Tgfbr2-cKO and reduced VEGFA secretion in *Tgfbr2* and *Foxg1* double knock-down cortical cells. (A) E13.5-derived cultured cells of Tgfbr2-cKO (grey bars) and controls (white bars) secreted less VEGFA at DIV4 in DT and VT as well as at DIV12 in DT and DIV8 in VT, as detected by ELISA ($n = 3$ DT, brown; $n = 4$ VT, pink). (B) MLEC assay revealed increased TGFβ levels in CM of Tgfbr2-cKO in DT at DIV4–12, but not in VT ($n = 4$). (C–F) VEGFA was localized inside the Golgi complex in DT and VT of Tgfbr2-cKO, whereas cells of controls displayed occasional staining outside the Golgi (white arrowheads). (G) CM of E13.5 cortical cells infected with shFoxg1 and shTgfbr2 secreted less VEGFA compared with shScrambled control at DIV16 as analysed by ELISA ($n = 4$). (H and I) Verification of knock-down of *Foxg1* and *Tgfbr2* in cortical cells confirmed via qRTPCR ($n = 4$). $Log_2$ of the fold change is given compared with shScrambled-infected cells. (J) Time line of infection regime of cortical cells with viral particles. On DIV1, viral particles were applied in a reduced medium volume (red arrow). Volume was increased to normal level on DIV2 (orange arrow). Selection with puromycin occurred after removal of viral particles on DIV4 (green arrow). Half medium changes followed every 4 days (blue arrows) until cells and CM were harvested on DIV16 (grey arrow). Data were analysed using unpaired student's *t*-test (A, B) and one-way ANOVA, followed by Sidak post-test (G–I). Scale bar: 5 μm.

development (53,54). We cultured HUVEC in medium mixed in a 1 : 1 ratio of normal HUVEC medium to CM from DT or VT cells of Tgfbr2-cKO (CM_cKO) and controls (CM_Ctrl), respectively. Control conditions were (1) 1 : 1 mixture of HUVEC to neural basal (NB) medium (H_NB), because HUVEC did not grow in NB alone, and (2) H_NB supplemented with VEGFA and FGF2 (H_NB_suppl), because both factors are generally added to HUVEC culture medium in established protocols. Cultivation of HUVEC in CM from control and *Tgfbr2*-deficient cells did not change their proliferation as revealed by similar rates of BrdU incorporation (Supplementary Material, Fig. S8D). HUVEC that were cultured on Matrigel and treated with CM_cKO formed tubes with significantly fewer branching points compared with CM from control animals and to H_NB_suppl control medium, corroborating our *in vivo* observations (Fig. 6A, Supplementary Material, Fig. S8F, G). To analyse whether reduced or increased secretion of different factors, which we found to be altered in Tgfbr2-cKOs *in vivo*, could rescue the branching defect, we supplemented the CM with these factors and analysed the number of branching points. First, we supplemented the CM with VEGFA and FGF2, which rescued the branching defect in CM_cKO but increased branching only slightly in CM_Ctrl (Fig. 6B, Supplementary Material, Fig. S8Fb, d, Gb, d). To analyse whether supplementation with VEGFA or FGF2 alone could also improve sprouting of HUVEC in CM_cKO, we added both factors separately to CM. VEGFA supplementation increased the branching of HUVEC cultured in CM_cKO in DT and VT, but we observed only a slight increase in tube formation after FGF2 addition (Fig. 6C, Supplementary Material, Fig. S8E). Supplementation of CM with TGFβ1 decreased branching of HUVEC in medium from controls and mutants. TGFβ applied to control medium (H_NB_suppl, black) also reduced the branching ability of HUVEC (Fig. 6D). Because the double stimulation with VEGFA and FGF2 as well as treatment with VEGFA alone rescued the branching phenotype of HUVEC cultured in CM_cKO, we concluded that reduced secretion of VEGFA could be one reason for the branching defect observed *in vivo*. Further, increased secretion of TGFβ from the DT in Tgfbr2-cKO might also impair angiogenesis *in vivo*.

### Altered secretion of soluble factors by Tgfbr2-cKO primary neural cells reduces vascular migration

Using real-time cell analysis (RTCA), we studied migration of HUVEC towards CM of both control and Tgfbr2-cKO and observed that migration was generally less compared with control conditions (H_NB_suppl) (Fig. 7A–C). HUVEC

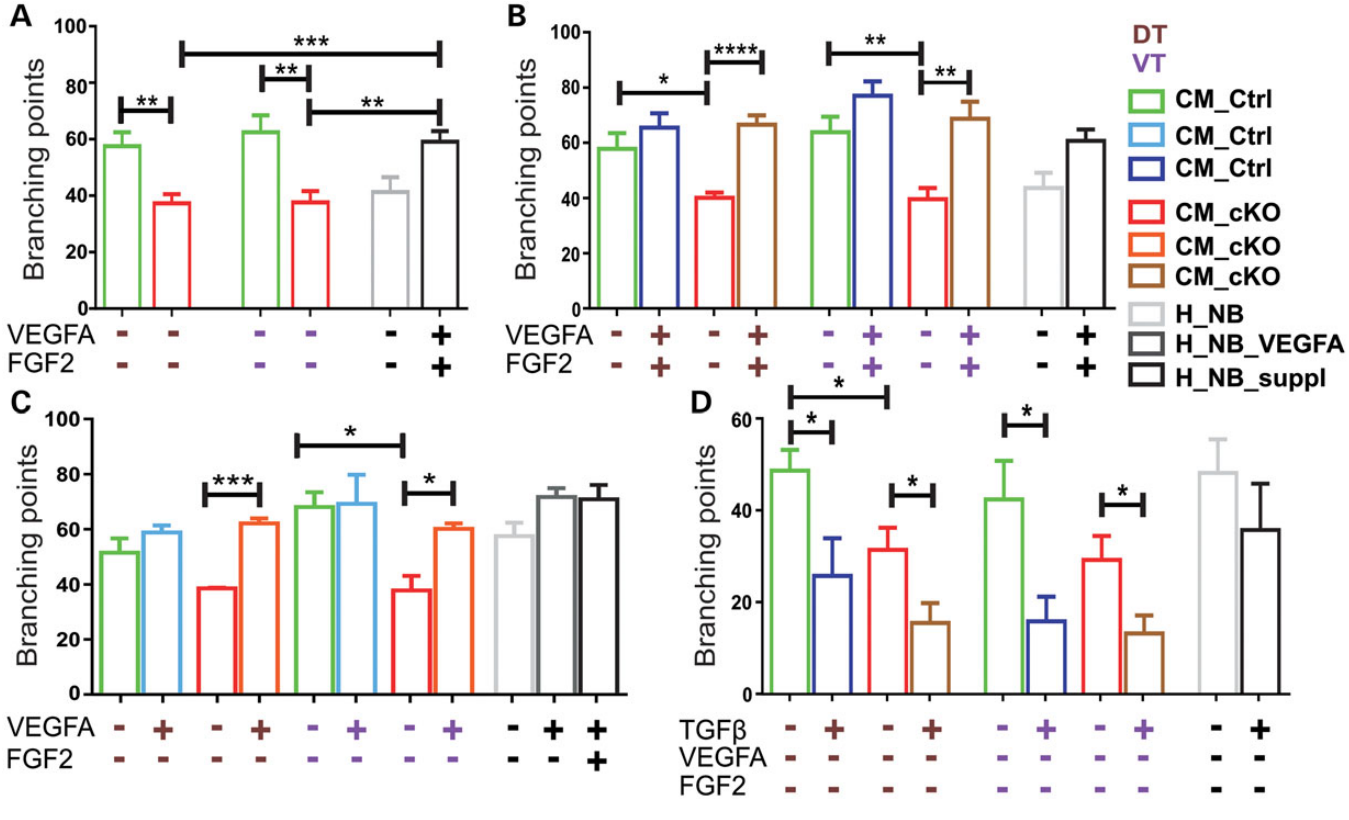


**Figure 6.** Impaired vascular branching of HUVEC treated with CM of Tgfbr2-cKO and rescue of the defect with VEGFA stimulation. (A) HUVEC cultured in CM_cKO (red, $n = 8$) had less branches compared with CM_Ctrl (green, $n = 8$). HUVEC showed increased branching under control condition H_NB_suppl (black) that stimulated angiogenesis, compared with unstimulated control condition H_NB (grey, $n = 7$). (B) VEGFA/FGF2 supplementation of CM_cKO rescued the branching defect (brown, $n = 7$), but only slightly increased sprouting in CM_Ctrl (blue, $n = 7$). Branching was increased when HUVEC were treated with VEGFA and FGF2 (H_NB_suppl) compared with the unstimulated condition (H_NB) ($n = 6$). (C) VEGFA supplementation rescued sprouting defects in CM_cKO (orange, $n = 3$) and slightly improved branching in CM_Ctrl (light blue, $n = 3$) like in controls ($n = 2$). (D) TGFβ supplementation reduced branching in CM_Ctrl (blue, $n = 4$), in CM_cKO (brown, $n = 4$) and in H_NB_suppl (grey, $n = 3$).

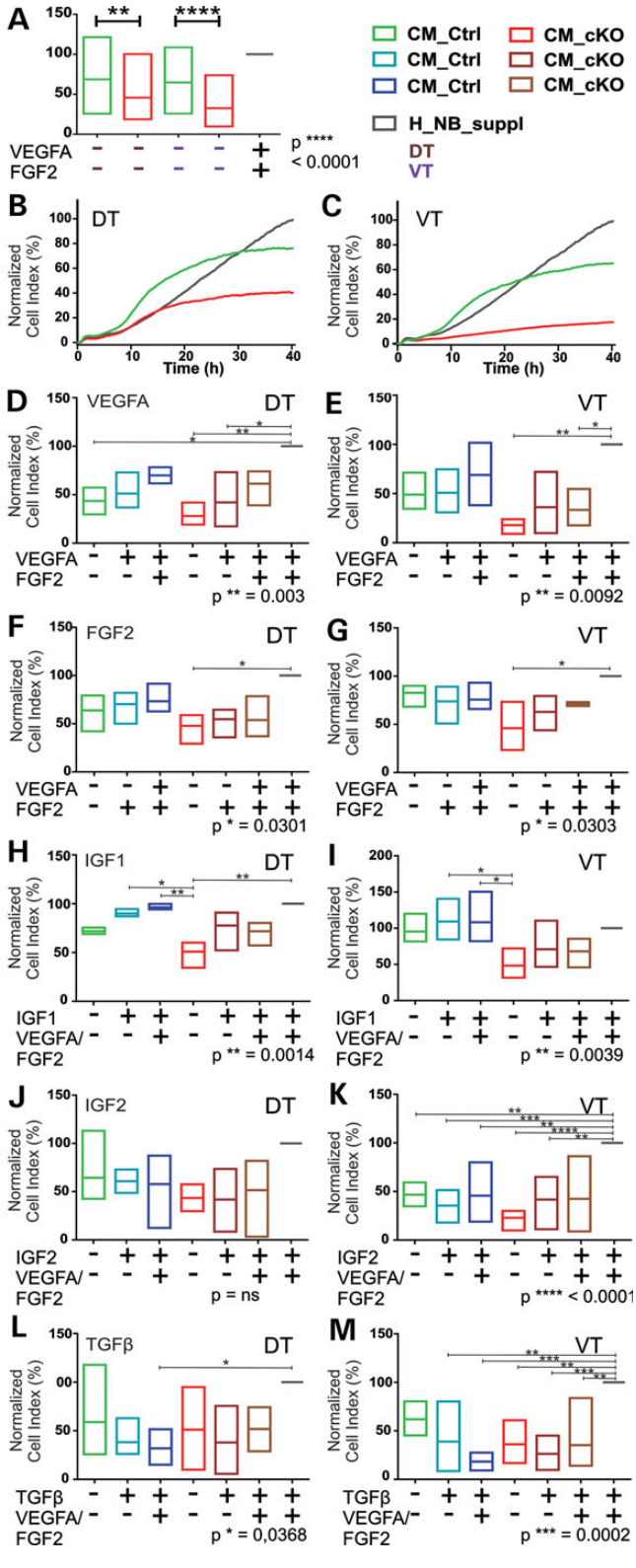


**Figure 7.** Impaired HUVEC migration through altered secretion of VEGFA, FGF2, IGF1, -2 and TGFβ. (A) Box-plot of end-point analyses of RTCA revealed reduced migration of HUVEC towards CM_cKO (red) compared with CM_Ctrl (green) of DT and VT ($n = 20$). The values for H_NB_suppl were set to 100% to normalize between different experiments and are therefore represented as an invariant grey line. (B and C) Growth curves of one representative experiment from DT and VT, respectively. Red line: CM_cKO, green line: CM_ctrl, grey line: H_NB_suppl control condition. (D and E) Box-plot representation of RTCA end-point analyses after supplementation with VEGFA alone, or in combination with FGF2. Addition of VEGFA alone rescued migration towards CM_cKO in VT-derived samples, but not in DT-derived samples (dark red). This is indicated by the loss of a significant difference between the treatment and control condition. Combined addition of VEGFA and FGF2 rescued migration in DT-derived samples, but not in VT-derived samples (light brown) ($n = 3$ for all experiments). (F and G) Box-plot of RTCA end-point analyses after supplementation with FGF2 alone or in combination with VEGFA. Addition of FGF2 rescued migration towards both VT- and DT-derived CM_cKO (dark red and light brown), also in the presence of VEGFA ($n = 3$ for all experiments). (H and I) Box-plot of RTCA end-point analyses after IGF1 addition rescued migration in DT-derived medium but had no significant effect in VT-derived medium (dark red). Combined addition of IGF1 with VEGFA and FGF2 did not improve migration further (light brown) ($n = 3$ DT, $n = 4$ VT). (J and K) Box-plot of RTCA end-point analyses after IGF2 supplementation. IGF2 addition alone did not rescue migration towards CM_cKO from both sources. Combined addition of IGF2 with VEGFA and FGF2 rescued in VT-derived CM_cKO ($n = 4$ DT, $n = 5$ VT). (L–M) Box-plot of end-point analyses after TGFβ1 supplementation, which impaired migration in the CM_Ctrl conditions, most strikingly in the presence of VEGFA and FGF2 (light and dark blue, $n = 4$). Data in A–M were normalized to H_NB_suppl (grey) of the respective experiment. All data were analysed by one-way ANOVA, followed by Sidak post-test.

showed reduced chemotaxis towards Tgfbr2-cKO CM as compared with CM from controls. CM_cKO from VT interfered even more with migration in comparison with CM from DT (Fig. 7A–C). To study the contribution of several factors independently, we supplemented the CM with VEGFA, FGF2, IGF1, -2, TGFβ1, THBS2 and ADAMTS1, respectively, and assessed for potential restoration of HUVEC migration. End-point analyses of several independent RTCA experiments revealed that double supplementation with VEGFA and FGF2 significantly increased HUVEC migration towards CM_cKO and thus rescued the defect (Fig. 7D–G, Supplementary Material, Fig. S9Ca, b). Supplementation of CM from control cells with VEGFA and FGF2 together significantly improved migration in DT-derived cells as well, but had no effect on migration when applied to VT-derived cells. We also assessed the contribution of each factor individually. Addition of VEGFA improved migration towards DT—but not towards VT-derived CM from Tgfbr2-cKO. Supplementation of DT-derived CM_cKO resulted in near complete rescue onto the CM_Ctrl level (Fig. 7D and E, Supplementary Material, Fig. S9Cc, d). Addition of FGF2 alone improved migration to cKO_DT/VT, but not up to non-supplemented Ctrl_DT/VT conditions (Fig. 7F and G, Supplementary Material, Fig. S9Ce, f). Hence, the best condition to restore migration ability in Tgfbr2-cKO was a double supplementation with VEGFA and FGF2. Next, we supplemented the CM with IGF1 and -2, as we had observed increased expression of these factors in Tgfbr2-cKO *in vivo*. IGF1 increased migration of HUVEC only towards DT-derived medium, whereas addition to VT-derived medium had only a moderate effect. In DT-derived CM_cKO, but not in VT-derived CM_cKO, IGF1 supplementation rescued HUVEC migration even above CM_Ctrl condition (Fig. 7H and I, Supplementary Material, Fig. S9Cg, h). Addition of IGF2 had little effect under control conditions (CM_Ctrl_DT/VT). However, in accordance with existing literature (55), increasing amounts of IGF2 in CM_Ctrl_VT also displayed the pro-angiogenic effects of IGF2 using the RTCA assay (Supplementary Material, Fig. S9Aa, b). In CM from

Tgfbr2_cKO, IGF2 improved migration towards VT-derived, but had no effect on DT-derived CM_cKO (Fig. 7J and K, Supplementary Material, Fig. S9Ci, j). *In vivo*, we discovered increased expression of IGF1 and -2 ligands. The potential to rescue the migration behaviour of HUVEC by addition of exogenous IGF in these experiments was therefore surprising. We hypothesized that bioavailability of the IGF ligands might be limited because of simultaneous increased expression levels of IGFBP2 and IGF2BP1, which might bind and sequester the IGF ligands. Addition of either IGFBP2 or IGF2BP1 did not have an observable impact on HUVEC migration towards mutant or control CM. Furthermore, the simultaneous addition of the ligands and binding proteins did not change migration behaviour (Supplementary Material, Fig. S9Da–d). These data suggested that the increased expression of IGFBP2 and IGF2BP1 did not contribute to impaired endothelial migration.

Supplementation of CM_cKO and CM_Ctrl in DT and VT with TGFβ1 revealed that excessive TGFβ1 interfered significantly with the migration of HUVEC towards these media (Fig. 7L and M, Supplementary Material, Fig. S9Ck, l). Whereas addition of TGFβ1 to CM_Ctrl_DT and VT significantly reduced the attraction towards this medium, further addition of TGFβ1 to CM_cKO did not aggravate the migratory defect. Stimulation with THBS2 did not affect HUVEC migration in DT or VT (Supplementary Material, Fig. S9Ba, b, e, f). ADAMTS1 supplementation showed slight region-specific differences. It reduced migration of HUVEC towards VT-derived control medium but did not interfere with HUVEC migration towards DT-derived Ctrl and cKO medium (Supplementary Material, Fig. S9Bc, d, g, h). Taken together, the addition of VEGFA, FGF2, IGF1 and -2 to cKO_DT/VT-derived CM improved angiogenesis of HUVEC and partially rescued the defective migration induced by CM of Tgfbr2-cKO. Increased secretion of TGFβ was another source that impaired angiogenesis of HUVEC. In conclusion with the altered secretion of VEGFA and TGFβ in cultured neural cells as well as our *in vivo* findings of VEGF protein aggregates, we elucidated strong evidence that alterations of VEGFA- and TGFβ-signalling are involved in the occurrence of haemorrhages in Tgfbr2-cKO.

## DISCUSSION

Transgenic mice with simultaneous ablation of TGFβ-signalling and reduction of FOXG1 in neural progenitors and neurons suffer from ICH mainly in the forebrain. We revealed impaired angiogenesis in terms of reduced branching and inhibition of proper EC migration owing to defective neural secretion in Tgfbr2-cKO, rather than defects in pericyte recruitment, endothelial cell proliferation or expression of cell junction proteins. Our study revealed altered expression and/or localization of pro-angiogenic factors, i.e. VEGFA, IGF1, -2, ID1, FGF2 as well as anti-angiogenic factors, i.e. IGFBP3, THBS2 and ADAMTS1. These data support the model that although pro-angiogenic signals are present within mutant forebrains, sprouting and consecutive migration of EC into the neural tissue is hampered, which results in the formation of disorganized cell clusters. Based on *in vitro* experiments using CM from cultured forebrain-derived cells to study EC-sprouting and -migration, we identified that VEGFA, FGF2 and TGFβ are main factors altered in mutant cells and that they impair proper sprouting and migration of HUVEC.

Angiogenesis within the forebrain originates from pial vessels that appear early in development, i.e. at E9 in the mouse (56). They may account for the fraction of normal vessels that we found in Tgfbr2-cKO forebrains as *Foxg1*-driven *cre*-expression is relatively weak in these early stages of development but strongly increases from E9.5 onwards (35). Sprouts from a second, periventricular network advance around E11 from the VT into the DT. At this stage, Tgfbr2-cKO did not display gross phenotypic abnormalities, but VEGFA already appeared in protein aggregates. This argues that initial angiogenesis from pial vessels is normal but that disturbances are associated with later embryonic stages in which periventricular vessels invade the forebrain. Haemorrhages in Tgfbr2-cKO appear first in the VT followed by the DT, and the phenotype is more pronounced in the VT. We provide data that show molecular differences between VT and DT in Tgfbr2-cKO. This includes differential secretion of TGFβ, differential expression of IGF-family members, differential capacity of IGF1 to rescue HUVEC migration, as well as differential expression of a variety of other proteins that we are currently investigating. Dorso-ventral (D/V) patterning of the forebrain is an evolutionary conserved process that starts around E10 in the mouse (57). Among the main signalling pathways implicated in D/V patterning are sonic hedgehog (SHH), wingless (WNT) and the TGFβ-superfamily, mainly through the function of BMPs. Involvement of the TGFβs themselves in the patterning is not reported, although they can exert divergent and specific functions also in other brain regions (58) or in different stages of development (59), emphasizing their context-dependent functions. D/V patterning is, however, under direct control of FOXG1, which influences signalling pathways by acting downstream of ventralizing SHH, or by inhibiting *Wnt8b*, *Tgfβ1* and *-2* transcription (60). As FOXG1 exerts different functions along the D/T axis, it is very likely that it is involved in the phenotypic variations that we observed between the VT and DT.

In a broader sense, our results indicate that early D/V patterning is not only necessary to specify domains to generate neurons that synthesize different neurotransmitters, i.e. glutamatergic, GABAergic or cholinergic neurons (61). In addition, regional differences are also implicated to direct simultaneous development of the nervous and the vascular system. Thus, different molecular compositions might be necessary to create adopted environments that allow migration and sprout development of blood vessels in a regionalized manner. This might be necessary to attract periventricular vessels to migrate from the VT into the DT. It is tempting to speculate, on the basis of our data, that regional differences in expression and/or bioavailability of VEGFA, IGF1, -2, TGFβ, THBS2 and ADAMTS1 are involved in this mechanism.

TGFβ-signalling in EC can be mediated through different receptor complexes. Whereas the TGFBR2 is an invariable component, two different type I receptors can be activated, namely ACVRL1/ALK1 and ALK5. There is strong indication that signalling via ALK1 activates SMAD1/5/8 with pro-angiogenic effects, i.e. stimulation of EC proliferation and migration. On the other hand, ALK5-signalling impinges on Smad2/3 that interferes with angiogenesis (62). One possibility to explain the inhibitory functions of TGFβ that we observed in our

branching and migration assays is that it is activating an ALK5-dependent EC response instead of ALK1. TGFβ has a higher affinity for ALK5 than ALK1 (63), and increased secretion in the DT might account for putative ALK5 activation. Another possibility is that the defective cellular or molecular environment of the EC in Tgfbr2-cKO includes proteins that induce the switch between both TGFβ pathways. Although we did not observe altered expression of ENG, other proteins, including LRG1 (64), might be affected. However, these hypotheses have to be studied in further analyses.

The *Foxg1-cre*-driven Tgfbr2-cKO is unique among mouse models with defective TGFβ-signalling in neural cells as it displayed a defective vasculature. Interference with TGFβ-signalling using other neural *cre*-lines does not result in ICH (40,41). Thus, reduction of FOXG1 together with *Tgfbr2* deletion seems causative for the observed phenotype. FOXG1 is implicated in modulating TGFβ-signalling and interferes with FOXO/SMAD-dependent transcription of cell cycle inhibitor *Cdkn1a* during CNS development (30,32). Apart from *Cdkn1a*, little is known about further FOXG1/SMAD-target genes. This study indicates that crosstalk of FOXG1 and TGFBR2-mediated signalling extends beyond *Cdkn1a* regulation and is not restricted to solely affect neuroepithelial cells.

EC that were hampered in their migration accumulated in clusters in Tgfbr2-cKO. This specific feature of impaired angiogenesis is also reported for other mouse lines, e.g. after deletion of TGFβ ligands in the entire forebrain (65,66), deletions of TGFBR2 in EC (26,41), upon knock-out of *ItgaV* or *Itgb8* in the neuroepithelium (67,68) and after deletion of *Gpr124* (27–29). *Gpr124* is transcriptionally activated through TGFβ and modulates TGFβ-signalling itself (27). In contrast, interference with SMAD4 expression in EC does not result in EC clusters, but in defective recruitment of pericytes (25). Mechanisms and molecular cues behind the formation of EC clusters are as yet hardly studied. Our data provide evidence that part of the phenotype is caused by secreted neural factors. Decreased VEGFA expression does not cause EC clusters in GPR124-deficient mice as these mice rather show increased transcription of VEGFA itself or of its target genes (27,29). Further *in vitro* experiments support the view of VEGF independence (28), but bioavailability of VEGFA has not been studied in detail. VEGFA has also not been reported as a molecular cue responsible for EC clusters in EC-specific loss of TGFBR2. It is therefore likely that EC clusters arising after EC-specific interference with TGFβ-signalling might be independent of VEGFA. Increased IGF1 and ID3 transcription are also observed in *Gpr124*-knock-out mice (27), which might be factors involved in EC clustering. However, our *in vitro* data indicate that increasing amounts of IGF1 and -2 revert impaired EC migration. Expression of IGFBPs has not been reported for any of the other mouse models, and it cannot be ruled out that limited bioavailability of IGF1 and/or -2 is associated with the formation of EC clusters. It is, however, unlikely that altered expression of IGF1/ -2 alone is sufficient to induce EC clusters, as angiogenesis defects are not among reported phenotypes of IGF1/ -2 transgenic or knock-out mice (69). Drawing parallels with Tgfbr2-cKO mice, EC clusters in ITGAV- and ITGB8-deficient mice also result from knock-out in neural cells. EC clusters that appeared after loss of ITGB8 are associated with increased cell proliferation, vessel instability and increased branching. Although Tgfbr2-cKO and ITGB8-deficient mice share formation of EC clusters, we did not observe increased cell proliferation in Tgfbr2-cKO. We also identified reduced branching during angiogenesis, indicating involvement of a different molecular mechanism. A possible explanation lies in the reported differences in bioavailability of TGFβ ligands: whereas loss of ITGB8 results in reduced release of TGFβ (66,70), *Foxg1-cre*-mediated loss of neural TGFBR2 resulted in increased TGFβ-release. This is in accordance with the observation that TGFβ influences angiogenesis differently and that its effects are dependent on TGFβ concentration (22). Expression of integrins in Tgfbr2-cKO is under current investigation to exploit a putative role in this model of TGFβ-dependent angiogenesis.

TGFβ is known to crosstalk to other signalling pathways and to promote expression of other factors that influence angiogenesis, e.g. VEGF (71). In this context, simultaneous activation of VEGF-signalling and inhibition of TGFβ-signalling leads to increased angiogenesis (24). Among several genes that are affected by this alteration of cytokine signalling, *Itga5* expression levels were increased and this promoted EC sprouting. This suggests that TGFβ-activation interferes with strong activation of VEGF-signalling. Therefore, it is also possible that the inhibitory effects of TGFβ that we observed are mediated by the interference with VEGF-signalling.

The $Foxg1^{cre/+};Tgfbr2^{flox/flox}$ mice can serve as a model to advance understanding of the interaction between neural and angiogenic cells during brain development. It should be appreciated that this complex phenotype is caused by a plethora of factors with altered expression and/or activity. Dysregulation of angiogenesis is associated with several diseases of the CNS, e.g. HHT, CAA, stroke, cancers and haemorrhages in preterm infants. These pathologies involve disturbed TGFβ-signalling, and our findings might inspire novel therapeutic approaches.

## METHODS

### Mice

$Foxg1^{cre/+}$ animals were mated with floxed *Tgfbr2*. Animal welfare committees of the University of Freiburg and local authorities approved all animal experiments (registered license X11/09S).

### Dissection, cell isolation, culturing, conditioned medium

Embryonic brains of various stages were fixed in 4% PFA for histology, frozen in nitrogen for protein and RNA or cultured, as previously described (8). One millilitre of CM was harvested on DIV4 and DIV8, on DIV12 cells and medium were harvested. CM was mixed 1 : 1 : 1 from all collection time points.

### Infection with lentiviral particles

Cortical cells were plated and infected on DIV1 with 2.5 MOI of viral particles (Fig. 5J). The following constructs were used: shTgfbr2 TRCN0000294600 with -HPGK-PURO-CMV-TagRFP and shFoxg1 TRCN0000081746 with -HPGK-PURO-CMV-TGFP (Sigma). For production of viral particles and titre determination, see Supplementary Material.

### *In vitro* tube formation assay and real-time cell analysis

A total of $6.5 \times 10^4$ HUVEC were pre-treated with 50% CM from controls and mutants and 50% starvation medium (EBM, Lonza) with 1% FBS for 18 h. $2.5 \times 10^4$ cells per well were seeded onto Matrigel (BD Biosciences) and cultured with 50% CM and 50% HUVEC medium with 2% FBS and without VEGFA and FGF2 (CM_Ctrl or CM_cKO_DT/VT). In control conditions, NB with VEGFA and FGF2 (H_NB_suppl) and without (H_NB) replaced CM. Tubes were fixed after 4–6 h for 20 min with 4% PFA; four images (4×) were taken and branching points quantified (ImageJ). We used 0.5 ng/ml of VEGFA, 10 ng/ml of FGF2 (both used for normal cultivation of HUVEC as recommended by Pelobiotech) and 5 ng/ml of TGFβ. RTCA (ACEA Biosciences) with CIM-plate (OMNI Life Science) monitored cell migration. Lower chambers were filled with CM_Ctrl/cKO (DT/VT) and where indicated with 0.5 ng/ml of VEGFA (#PB-Z1000-20), 10 ng/ml of FGF2 (PB-C044-A, Pelobiotech), 10 nM of IGF1 (#167100-11-B, tebu-bio) and IGF2 (#167100-12-B, tebu-bio), 5 ng/ml of TGFβ1 (#167100-21-B, tebu-bio), 20 ng/ml of ADAMTS1 (#5867-AD-020, R&D Systems) and THBS2 (#1635-T2-050, R&D Systems), 20 nM of IGFBP2 (#797-B2-025, R&D Systems) and IGF2BP1 (#H00010642-P01, ABNOVA). Upper plates were attached and filled with H_NB_suppl. After incubation and background measurement, $2.5 \times 10^4$ HUVEC were seeded in upper chambers. H_NB without cells was used as negative and H_NB_suppl in lower chamber as positive control. Experiments were performed in duplicates. Cell index was recorded with 100 sweeps every 10 min followed by 100 sweeps every 15 min. For end-point analyses after 42 h, all samples of an experiment were normalized to the corresponding positive control condition (H_NB_suppl), which was set to 100% in each individual experiment. This condition is displayed as grey line in either the end-point analyses or in the representative migration curve.

### Statistics

Unpaired student's *t*-test was used; data are given as mean ± SEM, *P*-value $^{*}<0.05$, $^{**}<0.01$, $^{***}<0.001$ and $^{****}<0.0001$, if not indicated otherwise.

Additional Material and Methods are given in Supplementary Material.

## AUTHORS' CONTRIBUTIONS

N.H. and T.V. designed research; N.H., S.C.W., R.V., S.D.W., S.H. and D.R. performed research; J.P. and J.S.E. contributed to reagents/analytic tools; N.H., S.C.W., R.V., S.D.W., D.R., J.P. and T.V. analysed data; N.H. and T.V. wrote the paper.

## SUPPLEMENTARY MATERIAL

Supplementary Material is available at *HMG* online.

## ACKNOWLEDGEMENTS

The authors thank P. Schwartz and S. Nestel for electron microscopy, S. Liebner for MEEC and CLDN5, CLDN12 antibodies, M. Löffler for technical support and K. Unsicker for critical comments on the manuscript.

*Conflict of Interest statement*. None declared.

## FUNDING

This work was supported by grants of Deutsche Forschungsgemeinschaft (grant number VO1676/1-1 to T.V.) and Forschungskommission der medizinischen Fakultät der Albert-Ludwigs-Universität Freiburg (to T.V.) and Stiftung der Deutschen Wirtschaft (to N.H.). S.C.W. is member of the Deutsche Forschungsgemeinschaft Graduiertenkolleg 1104. Funding to pay the Open Access publication charges for this article was provided by grants of Deutsche Forschungsgemeinschaft.

## REFERENCES

1. Goumans, M.J. and Mummery, C. (2000) Functional analysis of the TGFbeta receptor/Smad pathway through gene ablation in mice. *Int. J. Develop. Biol.*, **44**, 253–265.
2. Dünker, N. and Krieglstein, K. (2000) Targeted mutations of transforming growth factor-beta genes reveal important roles in mouse development and adult homeostasis. *Eur. J. Biochem. FEBS*, **267**, 6982–6988.
3. Derynck, R. and Zhang, Y.E. (2003) Smad-dependent and Smad-independent pathways in TGF-beta family signalling. *Nature*, **425**, 577–584.
4. Groppe, J., Hinck, C.S., Samavarchi-Tehrani, P., Zubieta, C., Schuermann, J.P., Taylor, A.B., Schwarz, P.M., Wrana, J.L. and Hinck, A.P. (2008) Cooperative assembly of TGF-beta superfamily signaling complexes is mediated by two disparate mechanisms and distinct modes of receptor binding. *Mol. Cell*, **29**, 157–168.
5. Li, M.O., Wan, Y.Y., Sanjabi, S., Robertson, A.-K.L. and Flavell, R.A. (2006) Transforming growth factor-beta regulation of immune responses. *Ann. Rev. Immunol.*, **24**, 99–146.
6. Wu, M.Y. and Hill, C.S. (2009) Tgf-beta superfamily signaling in embryonic development and homeostasis. *Develop. Cell*, **16**, 329–343.
7. Zhang, L., Zhou, F. and Ten Dijke, P. (2013) Signaling interplay between transforming growth factor-β receptor and PI3 K/AKT pathways in cancer. *Trends Biochem. Sci.*, **38**, 612–620.
8. Jakobsson, L. and van Meeteren, L.A. (2013) Transforming growth factor β family members in regulation of vascular function: in the light of vascular conditional knockouts. *Experim. Cell Res.*, **319**, 1264–1270.
9. Pardali, E., Goumans, M.-J. and Ten Dijke, P. (2010) Signaling by members of the TGF-beta family in vascular morphogenesis and disease. *Trends Cell Biol.*, **20**, 556–567.
10. Gallione, C.J., Repetto, G.M., Legius, E., Rustgi, A.K., Schelley, S.L., Tejpar, S., Mitchell, G., Drouin, E., Westermann, C.J.J. and Marchuk, D.A. (2004) A combined syndrome of juvenile polyposis and hereditary haemorrhagic telangiectasia associated with mutations in MADH4 (SMAD4). *Lancet*, **363**, 852–859.
11. Loeys, B.L., Schwarze, U., Holm, T., Callewaert, B.L., Thomas, G.H., Pannu, H., De Backer, J.F., Oswald, G.L., Symoens, S., Manouvrier, S. *et al.* (2006) Aneurysm syndromes caused by mutations in the TGF-beta receptor. *New Eng. J. Med.*, **355**, 788–798.
12. Prigoda, N.L., Savas, S., Abdalla, S.A., Piovesan, B., Rushlow, D., Vandezande, K., Zhang, E., Ozcelik, H., Gallie, B.L. and Letarte, M. (2006) Hereditary haemorrhagic telangiectasia: mutation detection, test sensitivity and novel mutations. *J. Med. Genet.*, **43**, 722–728.
13. Ballabh, P. (2010) Intraventricular hemorrhage in premature infants: mechanism of disease. *Pediatric Res.*, **67**, 1–8.
14. Merhar, S. (2012) Biomarkers in neonatal posthemorrhagic hydrocephalus. *Neonatology*, **101**, 1–7.
15. Jiang, N., Li, X., Qi, T., Guo, S., Liang, F. and Huang, Z. (2011) Susceptible gene single nucleotide polymorphism and hemorrhage risk in patients with brain arteriovenous malformation. *J. Clin. Neurosci.*, **18**, 1279–1281.

16. Wyss-Coray, T., Lin, C., Sanan, D.A., Mucke, L. and Masliah, E. (2010) Chronic overproduction of transforming growth factor-β1 by astrocytes promotes Alzheimer's disease-like microvascular degeneration in transgenic mice. *Am. J. Pathol.*, **156**, 139–150.
17. Nassiri, F., Cusimano, M.D., Scheithauer, B.W., Rotondo, F., Fazio, A., Yousef, G.M., Syro, L.V., Kovacs, K. and Lloyd, R.V. (2011) Endoglin (CD105): a review of its role in angiogenesis and tumor diagnosis, progression and therapy. *Anticancer Res.*, **31**, 2283–2290.
18. Goumans, M.-J., Valdimarsdottir, G., Itoh, S., Rosendahl, A., Sideras, P. and Ten Dijke, P. (2002) Balancing the activation state of the endothelium via two distinct TGF-beta type I receptors. *EMBO J.*, **21**, 1743–1753.
19. Lamouille, S., Mallet, C., Feige, J.-J. and Bailly, S. (2002) Activin receptor-like kinase 1 is implicated in the maturation phase of angiogenesis. *Blood*, **100**, 4495–4501.
20. Lebrin, F., Goumans, M.-J., Jonker, L., Carvalho, R.L.C., Valdimarsdottir, G., Thorikay, M., Mummery, C., Arthur, H.M. and Ten Dijke, P. (2004) Endoglin promotes endothelial cell proliferation and TGF-beta/ALK1 signal transduction. *EMBO J.*, **23**, 4018–4028.
21. Pece-Barbara, N. (2005) Endoglin null endothelial cells proliferate faster and are more responsive to transforming growth factor 1 with higher affinity receptors and an activated Alk1 pathway. *J. Biol. Chem.*, **280**, 27800–27808.
22. Orlova, V.V., Liu, Z., Goumans, M.-J. and Ten Dijke, P. (2011) Controlling angiogenesis by two unique TGF-β type I receptor signaling pathways. *Histol. Histopathol.*, **26**, 1219–1230.
23. Pepper, M.S. (1997) Transforming growth factor-beta: vasculogenesis, angiogenesis, and vessel wall integrity. *Cytokine Growth Factor Rev.*, **8**, 21–43.
24. Liu, Z., Kobayashi, K., van Dinther, M., van Heiningen, S.H., Valdimarsdottir, G., van Laar, T., Scharpfenecker, M., Lowik, C.W.G.M., Goumans, M.J., Dijke, P.T. *et al.* (2009) VEGF and inhibitors of TGF type-I receptor kinase synergistically promote blood-vessel formation by inducing 5-integrin expression. *J. Cell Sci.*, **122**, 3294–3302.
25. Li, F., Lan, Y., Wang, Y., Wang, J., Yang, G., Meng, F., Han, H., Meng, A., Wang, Y. and Yang, X. (2011) Endothelial Smad4 maintains cerebrovascular integrity by activating N-cadherin through cooperation with Notch. *Develop. Cell*, **20**, 291–302.
26. Allinson, K.R., Lee, H.S., Fruttiger, M., McCarty, J. and Arthur, H.M. (2012) Endothelial expression of TGFβ type II receptor is required to maintain vascular integrity during postnatal development of the central nervous system. *PLoS ONE*, **7**, e39336.
27. Anderson, K.D., Pan, L., Yang, X.-m., Hughes, V.C., Walls, J.R., Dominguez, M.G., Simmons, M.V., Burfeind, P., Xue, Y., Wei, Y. *et al.* (2011) Angiogenic sprouting into neural tissue requires Gpr124, an orphan G protein-coupled receptor. *Proc. Natl Acad. Sci. USA*, **108**, 2807–2812.
28. Kuhnert, F., Mancuso, M.R., Shamloo, A., Wang, H.-T., Choksi, V., Florek, M., Su, H., Fruttiger, M., Young, W.L., Heilshorn, S.C. *et al.* (2010) Essential regulation of CNS angiogenesis by the orphan G protein-coupled receptor GPR124. *Science*, **330**, 985–989.
29. Cullen, M., Elzarrad, M.K., Seaman, S., Zudaire, E., Stevens, J., Yang, M.Y., Li, X., Chaudhary, A., Xu, L., Hilton, M.B. *et al.* (2011) GPR124, an orphan G protein-coupled receptor, is required for CNS-specific vascularization and establishment of the blood-brain barrier. *Proc. Natl Acad. Sci. USA*, **108**, 5759–5764.
30. Seoane, J., Le, H.-V., Shen, L., Anderson, S.A. and MassaguE, J. (2004) Integration of Smad and forkhead pathways in the control of neuroepithelial and glioblastoma cell proliferation. *Cell*, **117**, 211–223.
31. Siegenthaler, J.A., Tremper-Wells, B.A. and Miller, M.W. (2007) Foxg1 haploinsufficiency reduces the population of cortical intermediate progenitor cells: effect of increased p21 expression. *Cereb. cortex*, **18**, 1865–1875.
32. Siegenthaler, J.A. and Miller, M.W. (2008) Generation of Cajal–Retzius neurons in mouse forebrain is regulated by transforming growth factor β-Fox signaling pathways. *Develop. Biol.*, **313**, 35–46.
33. Vogel, T., Ahrens, S., Buttner, N. and Krieglstein, K. (2010) Transforming growth factor promotes neuronal cell fate of mouse cortical and hippocampal progenitors in vitro and in vivo: identification of Nedd9 as an essential signaling component. *Cereb. cortex*, **20**, 661–671.
34. Farkas, L.M., Dünker, N., Roussa, E., Unsicker, K. and Krieglstein, K. (2003) Transforming growth factor-beta(s) are essential for the development of midbrain dopaminergic neurons in vitro and in vivo. *J. Neurosci.*, **23**, 5178–5186.
35. Hébert, J.M. and McConnell, S.K. (2000) Targeting of cre to the Foxg1 (BF-1) locus mediates loxP recombination in the telencephalon and other developing head structures. *Develop. Biol.*, **222**, 296–306.
36. Xuan, S., Baptista, C.A., Balas, G., Tao, W., Soares, V.C. and Lai, E. (1995) Winged helix transcription factor BF-1 is essential for the development of the cerebral hemispheres. *Neuron*, **14**, 1141–1152.
37. Hanashima, C. (2004) Foxg1 suppresses early cortical cell fate. *Science*, **303**, 56–59.
38. Miyoshi, G. and Fishell, G. (2012) Dynamic Foxg1 expression coordinates the integration of multipolar pyramidal neuron precursors into the cortical plate. *Neuron*, **74**, 1045–1058.
39. Martynoga, B., Morrison, H., Price, D.J. and Mason, J.O. (2005) Foxg1 is required for specification of ventral telencephalon and region-specific regulation of dorsal telencephalic precursor proliferation and apoptosis. *Develop. Biol.*, **283**, 113–127.
40. Falk, S., Wurdak, H., Ittner, L., Ille, F., Sumara, G., Schmid, M., Draganova, K., Lang, K., Paratore, C., Leveen, P. *et al.* (2008) Brain area-specific effect of TGF-β signaling on Wnt-dependent neural stem cell expansion. *Cell Stem Cell*, **2**, 472–483.
41. Nguyen, H.-L., Lee, Y.J., Shin, J., Lee, E., Park, S.O., McCarty, J.H. and Oh, S.P. (2011) TGF-β signaling in endothelial cells, but not neuroepithelial cells, is essential for cerebral vascular development. *Lab. Invest.*, **91**, 1554–1563.
42. Eagleson, K.L., Schlueter McFadyen-Ketchum, L.J., Ahrens, E.T., Mills, P.H., Does, M.D., Nickols, J. and Levitt, P. (2007) Disruption of Foxg1 expression by knock-in of Cre recombinase: Effects on the development of the mouse telencephalon. *Neuroscience*, **148**, 385–399.
43. Watanabe, K., Kamiya, D., Nishiyama, A., Katayama, T., Nozaki, S., Kawasaki, H., Watanabe, Y., Mizuseki, K. and Sasai, Y. (2005) Directed differentiation of telencephalic precursors from embryonic stem cells. *Nat. Neurosci.*, **8**, 288–296.
44. Stubbs, D., DeProto, J., Nie, K., Englund, C., Mahmud, I., Hevner, R. and Molnar, Z. (2009) Neurovascular congruence during cerebral cortical development. *Cereb. cortex*, **19**, i32–i41.
45. Gerhardt, H., Golding, M., Fruttiger, M., Ruhrberg, C., Lundkvist, A., Abramsson, A., Jeltsch, M., Mitchell, C., Alitalo, K., Shima, D. *et al.* (2003) VEGF guides angiogenic sprouting utilizing endothelial tip cell filopodia. *J. Cell Biol.*, **161**, 1163–1177.
46. Lyden, D., Young, A.Z., Zagzag, D., Yan, W., Gerald, W., O'Reilly, R., Bader, B.L., Hynes, R.O., Zhuang, Y., Manova, K. *et al.* (1999) Id1 and Id3 are required for neurogenesis, angiogenesis and vascularization of tumour xenografts. *Nature*, **401**, 670–677.
47. Mitchell, D., Pobre, E.G., Mulivor, A.W., Grinberg, A.V., Castonguay, R., Monnell, T.E., Solban, N., Ucran, J.A., Pearsall, R.S., Underwood, K.W. *et al.* (2010) ALK1-Fc inhibits multiple mediators of angiogenesis and suppresses tumor growth. *Mol. Cancer Therapeutics*, **9**, 379–388.
48. Moya, I.M., Umans, L., Maas, E., Pereira, P.N.G., Beets, K., Francis, A., Sents, W., Robertson, E.J., Mummery, C.L., Huylebroeck, D. *et al.* (2012) Stalk cell phenotype depends on integration of Notch and Smad1/5 signaling cascades. *Develop. Cell*, **22**, 501–514.
49. Valdimarsdottir, G., Goumans, M.-J., Rosendahl, A., Brugman, M., Itoh, S., Lebrin, F., Sideras, P. and Ten Dijke, P. (2002) Stimulation of Id1 expression by bone morphogenetic protein is sufficient and necessary for bone morphogenetic protein-induced activation of endothelial cells. *Circulation*, **106**, 2263–2270.
50. Armstrong, L.C. and Bornstein, P. (2003) Thrombospondins 1 and 2 function as inhibitors of angiogenesis. *Matrix boil.*, **22**, 63–71.
51. Krady, M.M., Zeng, J., Yu, J., MacLauchlan, S., Skokos, E.A., Tian, W., Bornstein, P., Sessa, W.C. and Kyriakides, T.R. (2008) Thrombospondin-2 modulates extracellular matrix remodeling during physiological angiogenesis. *Am. J. Pathol.*, **173**, 879–891.
52. Lee, N.V., Sato, M., Annis, D.S., Loo, J.A., Wu, L., Mosher, D.F. and Iruela-Arispe, M.L. (2006) ADAMTS1 mediates the release of antiangiogenic polypeptides from TSP1 and 2. *EMBO J.*, **25**, 5270–5283.
53. Langford, D., Hurford, R., Hashimoto, M., Digicaylioglu, M. and Masliah, E. (2005) Signalling crosstalk in FGF2-mediated protection of endothelial cells from HIV-gp120. *BMC Neurosci.*, **6**, 8.
54. Naik, P. and Cucullo, L. (2012) In vitro blood-brain barrier models: current and perspective technologies. *J. Pharmaceutical Sci.*, **101**, 1337–1354.
55. Maeng, Y.-S., Choi, H.-J., Kwon, J.-Y., Park, Y.-W., Choi, K.-S., Min, J.-K., Kim, Y.-H., Suh, P.-G., Kang, K.-S., Won, M.-H. *et al.* (2009) Endothelial progenitor cell homing: prominent role of the IGF2-IGF2R-PLCbeta2 axis. *Blood*, **113**, 233–243.

56. Vasudevan, A., Long, J.E., Crandall, J.E., Rubenstein, J.L.R. and Bhide, P.G. (2008) Compartment-specific transcription factors orchestrate angiogenesis gradients in the embryonic brain. *Nat. Neurosci.*, **11**, 429–439.
57. Campbell, K. (2003) Dorsal-ventral patterning in the mammalian telencephalon. *Curr. Opinion Neurobiol.*, **13**, 50–56.
58. Roussa, E. and Krieglstein, K. (2004) Induction and specification of midbrain dopaminergic cells: focus on SHH, FGF8, and TGF-? *Cell Tissue Res.*, **318**, 23–33.
59. Wahane, S.D., Hellbach, N., Prentzell, M.T., Weise, S.C., Vezzali, R., Kreutz, C., Timmer, J., Krieglstein, K., Thedieck, K. and Vogel, T. (2014) PI3K-p110-alpha-subtype-signalling mediates survival, proliferation and neurogenesis of cortical progenitor cells via activation of mTORC2. *J. Neurochem.*, doi:10.1111/jnc.12718.
60. Danesin, C., Peres, J.N., Johansson, M., Snowden, V., Cording, A., Papalopulu, N. and Houart, C. (2009) Integration of telencephalic Wnt and hedgehog signaling center activities by Foxg1. *Develop. Cell*, **16**, 576–587.
61. Wilson, S.W. and Rubenstein, J.L. (2000) Induction and dorsoventral patterning of the telencephalon. *Neuron*, **28**, 641–651.
62. Goumans, M.-J., Valdimarsdottir, G., Itoh, S., Lebrin, F., Larsson, J., Mummery, C., Karlsson, S. and Ten Dijke, P. (2003) Activin receptor-like kinase (ALK)1 is an antagonistic mediator of lateral TGFbeta/ALK5 signaling. *Mol. Cell*, **12**, 817–828.
63. ten Dijke, P., Yamashita, H., Ichijo, H., Franzén, P., Laiho, M., Miyazono, K. and Heldin, C.H. (1994) Characterization of type I receptors for transforming growth factor-beta and activin. *Science*, **264**, 101–104.
64. Wang, X., Abraham, S., McKenzie, J.A.G., Jeffs, N., Swire, M., Tripathi, V.B., Luhmann, U.F.O., Lange, C.A.K., Zhai, Z., Arthur, H.M. *et al.* (2013) LRG1 promotes angiogenesis by modulating endothelial TGF-β signalling. *Nature*, **499**, 306–311.
65. Arnold, T.D., Ferrero, G.M., Qiu, H., Phan, I.T., Akhurst, R.J., Huang, E.J. and Reichardt, L.F. (2012) Defective retinal vascular endothelial cell development as a consequence of impaired integrin alpha V beta 8-mediated activation of transforming growth factor-beta. *J. Neurosci.*, **32**, 1197–1206.
66. Mu, D., Cambier, S., Fjellbirkeland, L., Baron, J.L., Munger, J.S., Kawakatsu, H., Sheppard, D., Broaddus, V.C. and Nishimura, S.L. (2002) The integrin alpha(v)beta8 mediates epithelial homeostasis through MT1-MMP-dependent activation of TGF-beta1. *J. Cell Biol.*, **157**, 493–507.
67. McCarty, J.H. (2004) Selective ablation of v integrins in the central nervous system leads to cerebral hemorrhage, seizures, axonal degeneration and premature death. *Development*, **132**, 165–176.
68. Proctor, J.M. (2005) Vascular development of the brain requires 8 integrin expression in the neuroepithelium. *J. Neurosci.*, **25**, 9940–9948.
69. D'Ercole, A.J., Ye, P. and O'Kusky, J.R. (2002) Mutant mouse models of insulin-like growth factor actions in the central nervous system. *Neuropeptides*, **36**, 209–220.
70. Cambier, S., Gline, S., Mu, D.Z., Collins, R., Araya, J., Dolganov, G., Einheber, S., Boudreau, N. and Nishimura, S.L. (2005) Integrin alpha v beta 8-mediated activation of transforming growth factor-beta by perivascular astrocytes – an angiogenic control switch. *Am. J. Pathol.*, **166**, 1883–1894.
71. Ten Dijke, P. and Arthur, H.M. (2007) Extracellular control of TGFbeta signalling in vascular development and disease. *Nat. Rev. Mol. Cell Biol.*, **8**, 857–869.